Piled Raft Foundation Supporting a Supertall Building in Osaka Constructed by Top-Down Method

K. Yamashita[1], J. Hamada[1] and K. Hirakawa[2]
[1] *Takenaka Research and Development Institute, Takenaka Corporation, Chiba, Japan*
[2] *Design Department, Tokyo Head Office, Takenaka Corporation, Tokyo, Japan*
E-mail: yamashita.kiyoshi@takenaka.co.jp

ABSTRACT: This paper offers a case history of 300-m high building in Japan. Since the building has a five-story basement, a top-down method was adopted to carry out the underground construction works safely as well as to save construction time by simultaneous construction of the upper and the basement floors. To ensure high performance against strong earthquakes, piled raft foundation consisting of large-diameter bottom-enlarged cast-in-place concrete piles and steel H-piles built-in soil-cement wall (TSW) was employed as a cost-effective solution. In order to corroborate the foundation design, field monitoring on the settlement and the vertical load sharing between the piles and the raft was performed. Consequently, it was found that the foundation design was appropriate.

KEYWORDS: Supertall Building, Piled Raft Foundation, Top-down Method, Settlement, Load Sharing, Field Monitoring.

1. INTRODUCTION

In recent years, there has been an increasing recognition that the use of piles to reduce raft settlements can lead to considerable economy without compromising the safety and performance of the foundation (Poulos, 2001). Recently, piled raft foundations have been used for the foundations of Burj Khalifa in UAE, the world's tallest building of 828 m in height (Poulos and Bunce, 2008), and many other overseas supertall buildings of 300 m or higher. Also in Japan, piled rafts were used for high-rise buildings of 150 m or higher (Kono et al., 2008; Yamashita et al., 2011).

A 300-m high building called Abeno Harukas, located in Osaka City, was completed in November 2013 and started business in March 2014 (Figure 1). The building of sixty stories with a five-story basement is now the tallest and the first supertall building in Japan. To support the large structure load effectively as well as to ensure safety during deep excavation works and save construction time, piled raft foundation using a top-down method was employed. Several case histories of piled rafts supporting high-rise buildings constructed by the top-down method were reported (Katzenbach et al., 2000; Kono et al., 2008; Yamashita and Hamada, 2013). However, case histories on the monitoring of the settlement and load sharing between the piles and the raft are very limited. Furthermore, particularly in highly active seismic areas, it is required to develop more reliable seismic design methods for piled rafts. This paper presents design and performance of a piled raft foundation constructed by the top-down method supporting the 300-m high building, including performance-based design under strong earthquakes. To corroborate the foundation design, field monitoring was performed on the settlement and the load sharing between the piles and the raft.

Figure 1 View of 300-m high building (Photo by H. Suzuki)

2. GEOLOGICAL-GEOTECHNICAL CONDITIONS

The construction site is located on Pleistocene terrace surface of Uemachi plateau. The Uemachi plateau is 2 km wide and 10 km long, 10-23 meters above the sea level, running roughly north-south across the center of the Osaka Plain, of which the Uemachi fault exists near the western end, as shown in Figure 2(a) (Research Committee on GOB, 2002) and Figure 2(b) (Ichihara, 1993). The

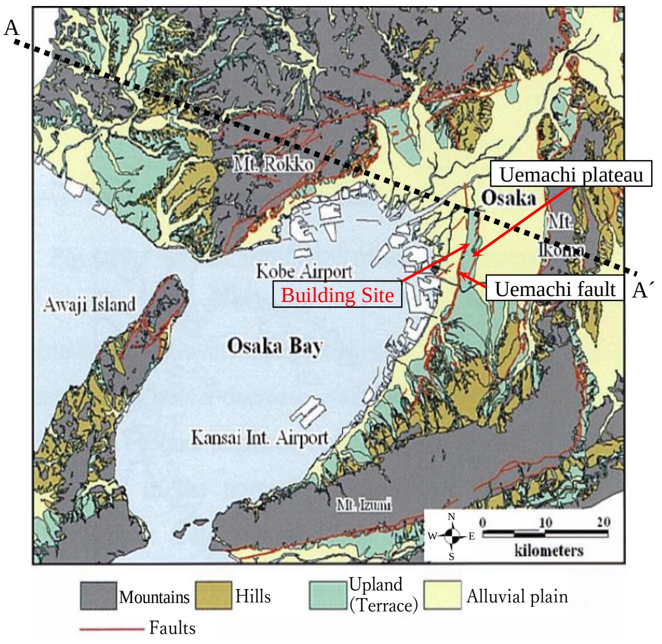

(a) Plan view of Osaka Plain

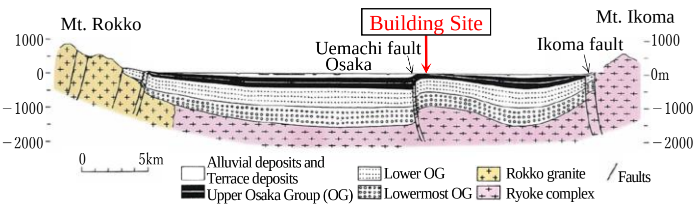

(b) East-west section of geological profile (Section A-A')

Figure 2 Geological map of Osaka Plain

site is located on the eastern side of the Uemachi fault. Pleistocene deposits, consisting of the terrace deposits and Osaka Group, were found below depths of 1-7 m from the ground surface based on the borehole survey (which was conducted outside of the site because there existed a building at that time). The Pleistocene deposits are supposed to be slightly inclined from the west to the east, hence, it is necessary to determine the pile toe depth considering the inclination of the deposits in the pile design.

3. BUILDING

3.1 Overview

The cross-section of the building in the NS direction and the foundation plan are illustrated in Figures 3 and 4, respectively. The building, approximately 71 m by 80m in plan, consists of a low-rise section, a mid-rise section, and a high-rise section, where the north facade is set back in steps as shown Figure 5. The major features of this building are as follows:

- Vertically integrated complex building including a railway terminal station, a department store, an art museum, offices, a hotel, an observatory and parking spaces
- High grade earthquake and wind resistant performance

To support the large axial loads acting on columns in the low-rise floors (and partly in the mid-rise floors), concrete filled steel tube (CFT) columns are used. The maximum nominal strength of the ultra-high strength concrete is 150 N/mm^2. The superstructure has truss at the top portion of the low-rise and mid-rise floors and just below the observatory.

To restrain the deformation of the superstructure, viscous oil dampers and rotational friction dampers are placed at the four corners in the low-rise floors. In the mid-rise floors, steel seismic braces are placed, moreover, outriggers of braces are provided to resist deformation due to bending. In the high-rise floors, the multi-story open space under the hat truss is equipped with core truss dampers in addition to the steel seismic braces. Furthermore, to improve the habitability of the hotel in strong winds, the hat truss floor has active tuned mass dampers (ATMD).

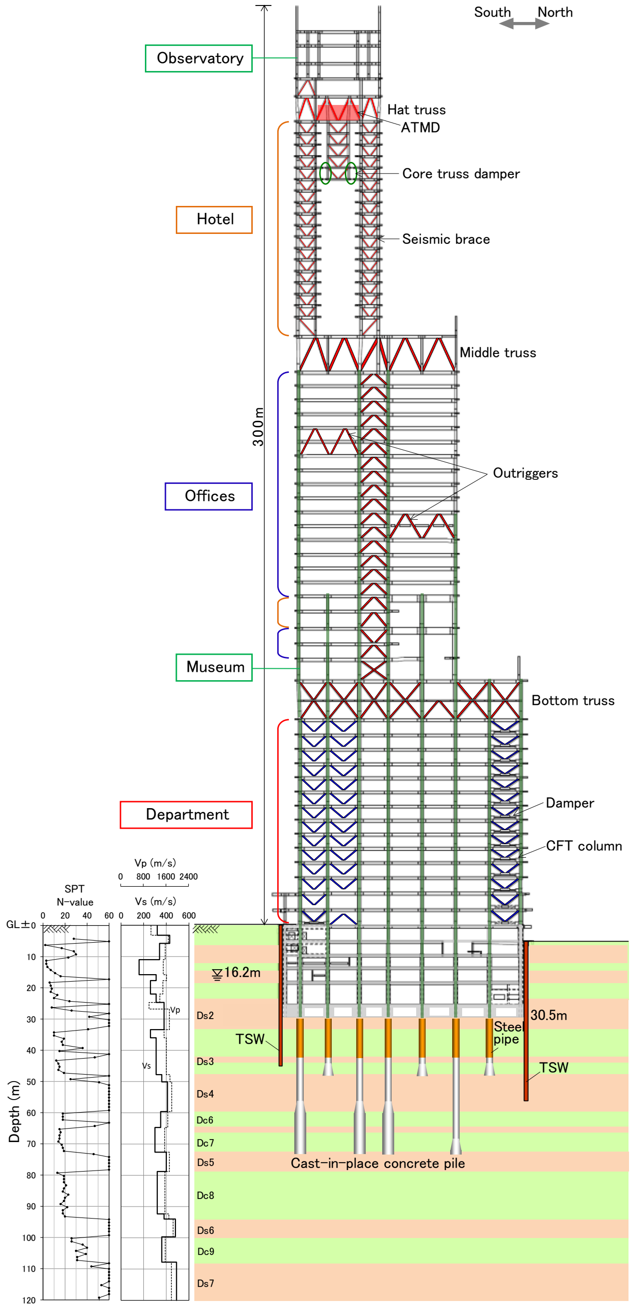

Figure 3 Cross-section of building and foundation (Street 5)

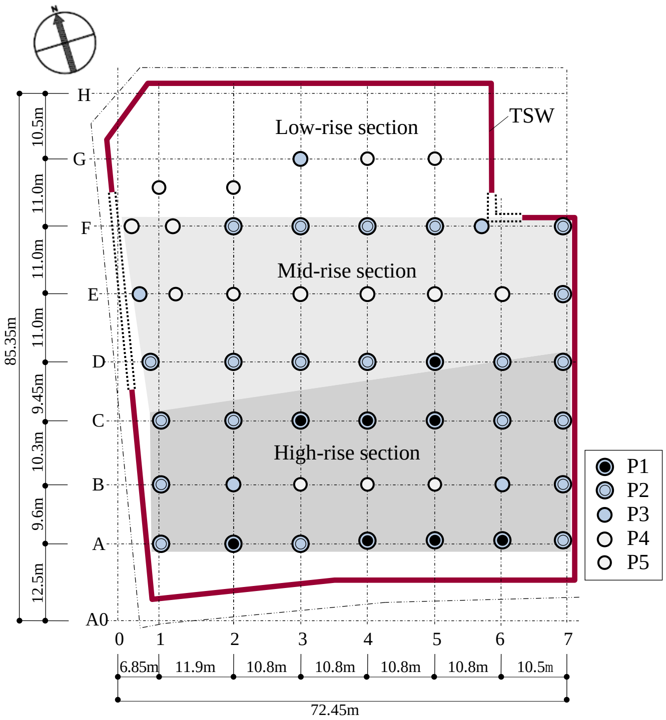

Figure 4 Foundation plan with layout of piles and TSW

Figure 5 Facade in west side (Photo by H. Suzuki)

Table 1 Seismic hazard and performance levels

Seismic hazard levels		Level 1	Level 2	SSMa Level
Frequency		Frequent	Rare	
Mean return period		Approx. 50 years	Approx. 500 years (Design-basis Earthquake)	(1.5 times stronger than Level 2)
Performance Levels		Continued Operation	Immediate Occupancy	Immediate Occupancy
Description		No damage	Minor damage	Minor damage
Requirements				
Superstructure	Inter-story drift angle (rad.)	5.0×10^{-3} or less	10.0×10^{-3} or less	13.5×10^{-3} or less
	Ductility factor of story	Allowable stress or less	1.0 or less	2.0 or less
Foundation (Piles)	Horizontal load	Damage limit state or less	Damage limit state or less	Below ultimate limit state
	Vertical load	Damage limit state or less (Factor of safety≥1.5)	Damage limit state or less (Factor of safety≥1.5)	Below ultimate limit state (Factor of safety≥1.2)

3.2 Seismic design of superstructure

Table 1 shows the seismic hazard and performance levels for the performance-based design, which is referred to Verdugo (2017). For the seismic design of high-rise buildings in Japan, the time-dependent input motions of artificial earthquakes on the engineering bedrock are generally used where the site effect could be taken into account. The acceleration response spectra of the artificial earthquakes should be compatible to the code-defined spectrum of Level 1 and 2 earthquakes shown in Figure 6 (The Building Standard Law of Japan, 2000). In addition to the artificial earthquake input motions, the actual seismic records (such as the 1940 El Centro, 1952 Taft and 1968 Hachinohe) with the calibrations upon a specified peak ground velocity (0.25 m/s for Level 1 and 0.50 m/s for Level 2) are used.

In the seismic design of this building, to upgrade seismic safety, a hazard level of seismic safety margin analysis level (referred as SSMa Level, hereafter) is introduced. The seismic intensity of SSMa Level is 1.5 times stronger than that considered in Level 2 earthquakes. Six site waves based on the active fault distribution in the area, historical earthquake activity and bedrock structure etc. are also used as the SSMa Level motions. Concerning the performance level under the SSMa Level motions, an occurrence of plastic hinges in the beams and braces is allowed while that in the columns is not allowed.

4. FOUNDATION DESIGN

The gross load in the structural design was 3,166 MN with its basement area of 5,362 m^2. The average pressure over the raft was 590 kPa (which is nearly equal to total stresses in basement excavation), and 716 kPa under the high-rise section. The piled raft consists of a raft and large diameter cast-in-place concrete piles. The raft, consisting of 4.5-m deep foundation beam and 1.0-m thick foundation slab with its bottom at 30.5 m depth, was embedded in Pleistocene very dense sand below a depth of 25 m (Ds2) as shown in Figure 3. The groundwater table of artesian head in the sand layer (Ds2) was found 16.2 m below the ground surface based on the in-situ permeability test result, while the water table was found around 6.7 m using dry boring.

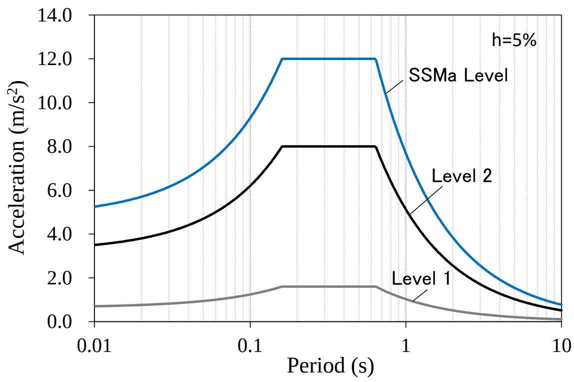

Figure 6 Acceleration response spectra on bedrock.

In addition to the cast-in-place concrete piles, steel H-piles built-in soil-cement wall (TSW) were placed along the outer perimeter of the basement frame. The layout and specifications of the piles and TSW are shown in Figure 4 and Table 2, respectively.

4.1 Piles

It is common in Japan that one column is supported by one pile and bottom-enlarged piles are employed in tall buildings to support the large axial loads. This arises probably because the geotechnical bearing capacity of piles defined in Japanese building design code depends significantly on the toe bearing capacity, rather than the shaft frictional resistance (Building Standard Law of Japan, 2000). Piles P1, P2 and P3 are placed under the columns supporting the large axial load of 45-80 MN under working load conditions. The pile toes reach the very dense sand (Ds5) below the depth of 70 m from the ground surface, while those of Piles P4 and P5 reach to the very dense sand (Ds4) below the depth of 45 m. The toe depths of Piles P1, P2 and P3 were varied from 70.5 to 73.1 m, considering the inclination of the layer (Ds5) based on the results of a couple of borehole survey (50 m away each other) as mentioned in Section 2. The construction method and quality control of the bottom-enlarged cast-in place concrete pile using high strength concrete (in which the

Table 2 Specifications of piles and TSW

	Column load (MN)	Shaft diameter (m)	Toe diameter* (m)	Toe depth (m)	Ultimate capacity (MN)	Concrete strength (N/mm^2)
P1	71.9-79.6	2.5	4.2 (4.1)	72.7-70.9	159	60
P2	46.7-74.0	2.5	4.2 (4.1)	73.1-70.5	140	60
P3	44.6-59.0	2.5	3.5 (3.4)	72.7-70.9	120	48
P4	33.5-48.1	2.5	3.5 (3.4)	48.2	94	48
P5	25.2-42.3	2.3	3.3 (3.2)	48.2	84	48
TSW	—	1.1 (wall width)	—	45.0-55.0 (steel H)	7.2-12.6 (MN/m)	2.0 (soil cement)

* Values in parentheses indicate those used in design.

nominal compressive strength is 60 N/mm^2 for Piles P1 and P2 and 48 N/mm^2 for Piles P3 to P5) were presented in detail by Hirai et al. (2015).

Figure 7(a) illustrates the cross-section of Pile P1. The ultimate geotechnical bearing capacity of Pile P1 was very large, 159 MN. Hence, a bottle-shaped enlarged pile toe (having a diameter of 4.2 m and a length of approximately 12 m) was employed to ensure the bearing capacity by making use of frictional resistance of the hard clay layers (Dc6 and Dc7). Piles P2 to P5 have a normal bottom-enlarged shape as shown in Figure 3. Although the pile toe of Piles P1 to P3 reach to the very dense sand (Ds5), the thickness of the sand is around 4 m (equal or less than the toe diameter) and there is a thick clayey soil (Dc8) below the pile toe. Thus, the toe bearing capacity of Piles P1 to P3 was determined (7.0 MPa) considering the bearing capacity and consolidation yield stress of the clayey soil.

4.2 TSW

Figure 7(b) illustrates the typical cross-section of TSW. The width of the soil-cement wall is 1.1 m and the center-to-center spacing of the steel-H members is 0.5 m. The axial load of the superstructure is transferred to the steel-H member (cross-section: 900×300×16×28 mm) in the soil-cement wall via the concrete basement wall using studs on the steel-H. Then, the axial load is transferred to the soil by frictional force between the soil-cement wall and the soil. The TSW has three types of steel-H member in which the length and the number of studs are varied according to the load.

The bearing capacity of TSW in design should be the minimum value of those calculated considering the following failure modes.

(a) Soil shear failure at the interface between the soil cement and the soil
(b) Bearing failure on the closed section of soil-cement core
(c) Bond failure caused by a slip on the core surface reinforced by the studs.

The bearing capacity of a single steel-H pile under the working load conditions was set to 1.2-2.1 MN. The steel-H pile was also designed to resist against the pulling load of 0.74 MN under Level 2 earthquakes. It was confirmed that the bearing capacity of the failure mode (a) was the minimum under both the working load and seismic conditions. In addition, to verify the design bearing capacity of TSW, a static compressive load test was performed.

The basement wall was designed as a hybrid one which consists of the steel-H members with the studs and the post-cast reinforced concrete basement wall. The design strength of the soil cement using the in-situ excavated soil was 2 N/mm^2. The safety of the steel-H members was examined by considering the residual stresses in the steel-H generated during the underground construction because the TSW was also used as an earth retaining wall.

4.3 Piled raft constructed by top-down method

The top-down method is a process of building substructure works after the construction of the 1st floor while superstructure works proceed simultaneously above as illustrated in Figure 8. In the top-down method, a preceding load which means a temporary construction load before the construction of raft at a bottom of the basement is supported solely by piles, while a subsequent load is supported by both the piles and raft (i.e., piled raft). Hence, the load carried by the piles and those carried by the raft are calculated as follows (Yamashita and Hamada, 2013).

For piled rafts, the equilibrium equation of the vertical loads is expressed by the equation (1).

$$W = P_p + P_r \quad (1)$$

where

W: gross load of structure
P_r: load carried by raft
P_p: load carried by piles

In the top-down method, the equilibrium equations for P_p and P_r are expressed by the equations (2) and (3).

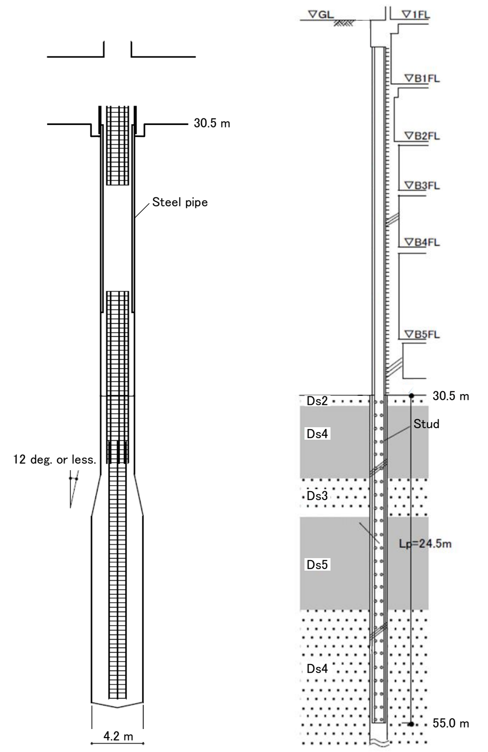

(a) Pile P1 (b) TSW

Figure 7 Cross-section of cast-in-place concrete pile and TSW

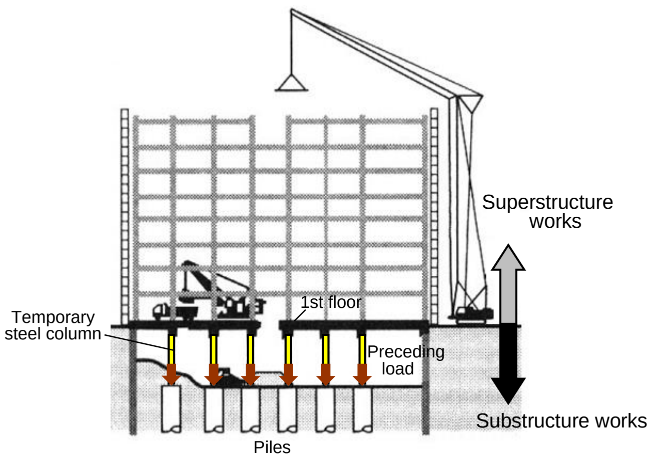

Figure 8 Schematic of top-down method

$$P_p = W_1 + \alpha_p'(W - W_1 - U_w) \quad (2)$$

$$P_r = (1 - \alpha_p')(W - W_1 - U_w) + U_w \quad (3)$$

where

W_1: preceding load
U_w: groundwater buoyancy acting on raft bottom
α_p': ratio of load carried by the piles to subsequent net load ($0<\alpha_p'<1$) where net load is gross load minus buoyancy

In addition, taking account of a weight of raft which is constructed before the buoyancy acts (denoted as W_2), the equations (2) and (3) are modified as the equations (4) and (5), respectively.

$$P_p = W_1 + \alpha_p'(W - W_1 - W_2 - U_w) \quad (4)$$

$$P_r = W_2 + (1 - \alpha_p')(W - W_1 - W_2 - U_w) + U_w \quad (5)$$

Based on the construction process, the preceding load was estimated to be 60% of the gross load considering that the superstructure frame would be constructed up to 55th floor at that time. For the subsequent load (40% of the gross load), the settlement and the load sharing between the piles and the raft were evaluated using a basement-raft frame model with springs of the piles and the soil. The vertical stiffnesses of piles and soil were determined using the simplified analysis method in consideration of the interaction among piles, soil and raft proposed by Yamashita et al. (1998). The soil shear modulus was determined as small strain shear modulus (obtained from the shear wave velocities derived from a P-S logging shown in Figure 3) multiplying a degradation factor. In general, soil shear modulus in the soil mass below the raft is degraded due to the increase in shear strains due to the stress release caused by the basement excavation as well as the subsequent load of raft and piles. In the top-down method, the soil shear modulus would be increased due to the increase in confining pressure in the soil mass which is caused by the preceding load via the piles. Then, the degradation factor was set at 0.5-0.7 empirically.

The ratio of the load carried by the piles (α_p') was computed as 0.66 (average value) using the simplified method, and the design value of α_p' was set to 0.75 by adding some margin to the computed value. Hence, the ratio of the load carried by the piles to the gross load was assumed to be 0.90 (i.e., 0.60+0.40x0.75), in which the groundwater buoyancy acting at the raft bottom was neglected in the pile design on a conservative side. On the other hand, although the ratio of the load carried by the raft to the gross load was given as 0.14 (i.e., 0.40x(1-0.66)) when the buoyancy was neglected, the foundation slab should be designed considering the water pressure acting on the raft bottom at 30.5 m depth. Using the water table of 6.7 m depth from the dry boring, the hydrostatic water pressure was assumed to be 235 kPa at the raft bottom.

4.4 Seismic design

In general, piled rafts can provide adequate capacities against the lateral and moment loads from the structure because the loads are carried by both the piles and raft. However, when the raft bottom is deep and the water table is high such as this building, no substantial effective contact pressure beneath the raft might be expected due to high water-pressure acting on the raft bottom. Then, in addition to the frictional resistance at the raft bottom, the passive earth pressure and side friction of the very dense sand (Ds2) acting on the basement walls were considered as a lateral resistance against the lateral forces. The total lateral resistance (878 MN), which is the sum of the frictional resistance at the raft bottom, the passive earth pressure and the side friction, was found to be sufficiently greater than the design horizontal load under Level 2 motions (490 MN).

Under Level 2 and the SSMa Level earthquake motions, kinematic effects on the sectional force of piles in piled raft arising from the lateral ground movements as well as inertial effects from the structure were considered. Tokimatsu et al. (2005) proposed that the pile stress may be given by the square root of the sum of the squares of the two sectional forces caused by the inertial and kinematic effects, provided that the inertial and kinematic forces are out of phase with each other and act on the pile separately. Since the primary natural period of the superstructure T_b (5.6-5.8 s) is fairly longer than the predominant period of the ground T_g (around 1.2 s), the bending moments of the piles were evaluated according to the proposal by Tokimatsu et al. (2005). The bending moments of the piles caused by the inertial force were computed using the simplified analysis method proposed by Hamada et al. (2015) in consideration of the lateral stiffness ratio of the piles to the basement walls on which the passive earth pressure and side friction act. The analysis result indicated that the ratio of the lateral load carried by the piles to the inertial force was 0.46 under Leve 2 motions. The bending moments caused by the kinematic effects were calculated using a pseudo-static analysis based on Beam-on-Winkler-springs method. The maximum relative ground displacement between the pile head and the pile toe (about 70 m depth) was approximately 50 mm. As a result, the maximum bending moments of 48-27 MNm at the pile head for Piles P1-P5 were obtained under Level 2 motions, where the bending moment caused by the inertial force was dominant.

The requirements for the piles are shown in Table 1. For the horizontal load, the damage limit state means that the unit stress at the edge of the concrete is virtually in the elastic condition while the ultimate limit state means that the unit stress at the edge of the concrete reaches the compressive strength. To ensure the target performance levels against the large bending moments, a steel pipe having an outer diameter of 2.3-2.5 m (14-25 mm in thickness) and a length of 12.5 m was provided for reinforcement of the top portion of the pile shaft. For the vertical load, a factor of safety against the ultimate bearing capacity under Level 2 earthquake was set to 1.5, while that under the SSMa level earthquake was set to 1.2. Note that a factor of safety for high-rise buildings in Japan is generally 1.2 under Level 2 earthquakes.

5. MONITORING

5.1 Instrumentation

In order to corroborate the foundation design, field monitoring on the settlements and the vertical load sharing between the piles and the raft was performed. The measurement items were vertical ground displacements below the raft, settlements of the 1st-floor, axial loads of CFT columns and contact pressure and pore-water pressure beneath the raft. The location of monitoring devices is illustrated in Figure 9. The settlement gauges were installed at the mid-point between the piles and the ground displacements were measured at three depths in reference to the point at 74.9 m depth.

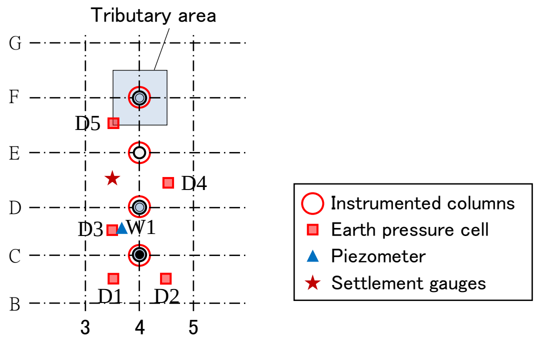

(a) Plan view

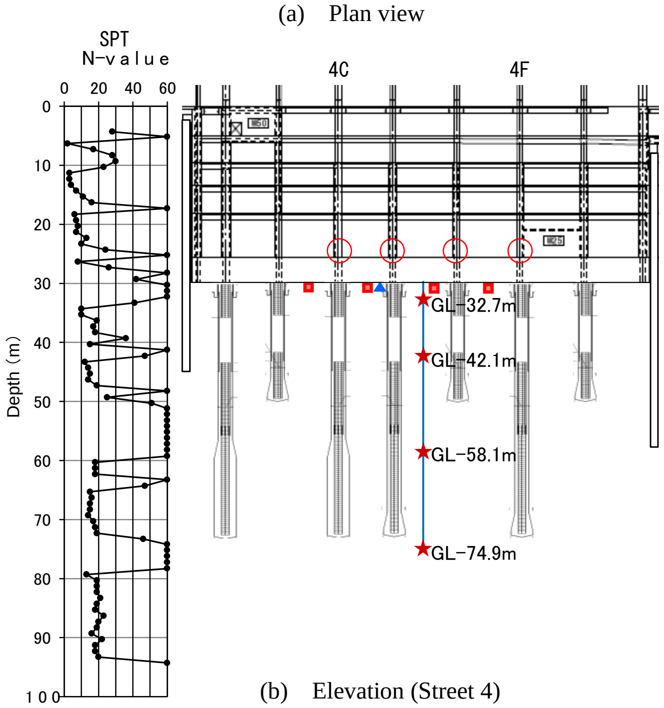

(b) Elevation (Street 4)

Figure 9 Location of monitoring devices

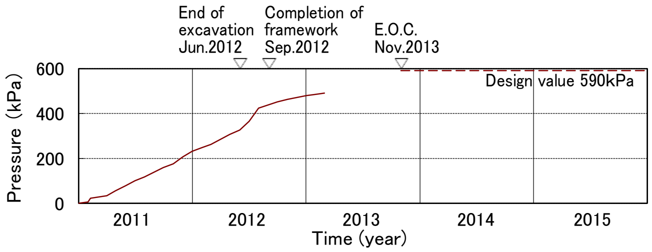

(a) Average pressure of structure load

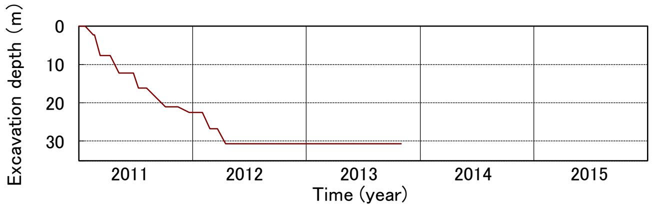

(b) Excavation depth

Figure 10 Structure load and excavation depth vs. time

The axial loads of the CFT columns were measured at 1.0 m above the 5th basement floor (just above the raft). The settlements of the 1st-floor columns were measured using an optical level where the reference point was set about 60 m away from the building.

5.2 Results of monitoring

5.2.1 Foundation settlements

Figure 10 shows the time-dependent average pressure of the structure load and excavation depth which were recorded according to the progress of construction. The average pressure was estimated using the construction records such as volume of concrete placing, weight of steel members, precast concrete of balcony and equipment instruments.

Figure 11 shows the development of the vertical ground displacement measured by the differential settlement gauges. Here, a negative sign means a rebound. The rebounds occurred as the excavation for the basement construction proceeded, and at the end of the excavation the maximum value of 47 mm was observed at 32.7 m depth. After the casting of the foundation slab, the settlement of the ground at 32.7 m depth (just below the raft) was approximately equal to that of the piled raft. The settlement of the piled raft due to the subsequent load was 7 mm in April 2013 when about 85% of the gross load was imposed on the foundation as is seen in Figure 10(a). Thereafter, the ground displacements at depths of 42.1 and 58.1 m were almost constant and quite stable, though the settlement gauge at 32.7 m depth ceased functioning. This suggests that no significant settlement of the piled raft occurred after that.

Figure 12 shows the measured settlements of the 1st floor columns at four points (3D, 4E, 4F and 7D) on February 2013. The settlements were 28-33 mm. Note that these settlements include the vertical displacements of the piles due to the preceding load and those of the piled raft due to the subsequent load, in addition, the axial shrinkage of CFT columns under the 1st floor. The computed settlements at the 1st floor in the design phase are also shown in Figure 12. The measured values suggest a uniform distribution while the computed values indicate reduced settlement on the both edges. This arises because stiffness of the basement frame and raft was neglected in the computation considering the top-down construction process. Nevertheless, the computed settlements roughly agreed with the measured ones while the former was slightly larger than the latter.

5.2.2 Load sharing between piles and raft

Figure 13 shows the development of the measured contact pressure and pore-water pressure underneath the raft. The contact pressures increased sharply due to raft construction and the subsequent

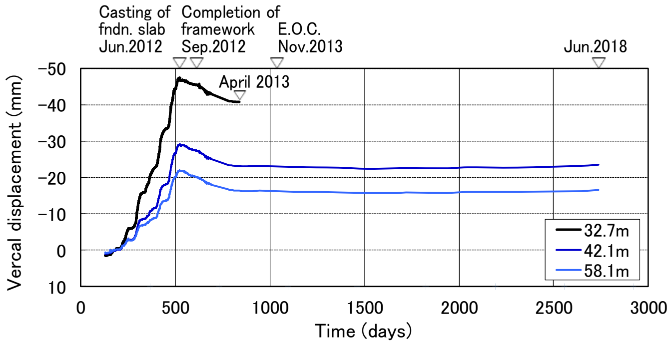

Figure 11 Measured vertical ground displacements in reference to the depth of 74.9 m

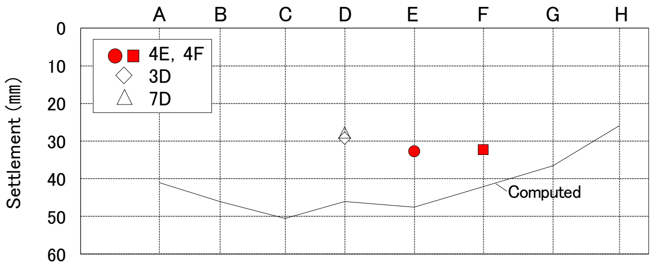

(a) Along Street 4

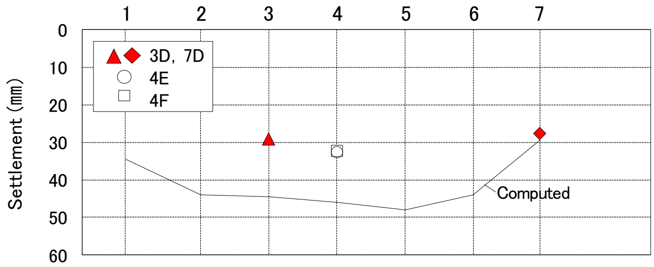

(b) Along Street D

Figure 12 Measured and computed settlement profiles at 1st floor (Feb. 22, 2013)

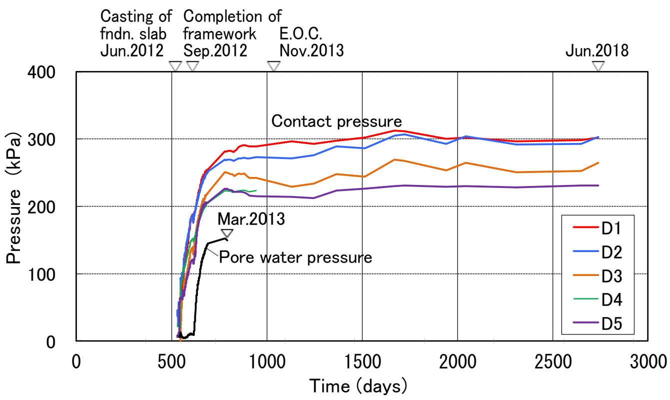

Figure 13 Measured contact pressure and pore-water pressure underneath the raft

increase in pore-water pressure acting on the raft bottom which was caused by the cease of pumping up. After the end of the construction in November 2013 (denoted as E.O.C., hereafter), the contact pressures were stable. The contact pressures around Column 4C (D1, D2 and D3) were 265-303 kPa and that around Column 4F (D5) was 231 kPa in June 2018, 55 months after E.O.C. The pore-water pressure was 150 kPa at the beginning of March 2013. The

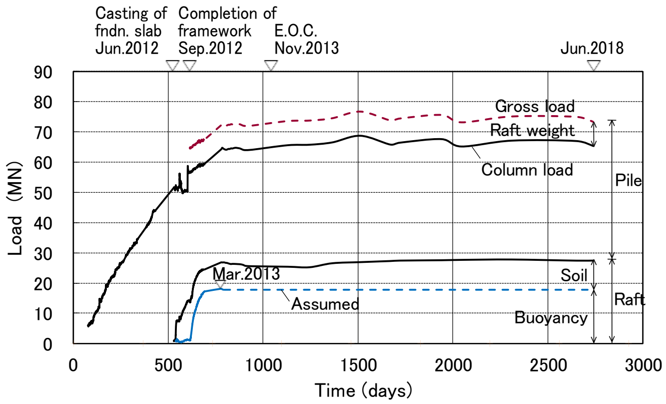

Figure 14 Load sharing between pile and raft in the tributary area of Column 4F

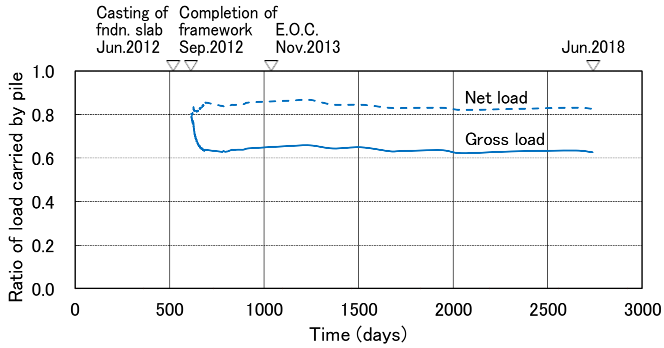

Figure 15 Ratio of load carried by pile after casting of raft

measured value was consistent with the artesian water pressure in the dense sand (Ds2) from the in-situ permeability test result (140 kPa at the depth of 30.5 m). Thereafter, the piezometer ceased functioning.

Figure 14 shows the time-dependent vertical load sharing among the pile, the soil and the buoyancy in the tributary area of Column 4F shown in Figure 9(a). In June 2018, the measured axial load of Column 4F was 65.4 MN. The gross load in the tributary area was estimated by adding a weight of the raft below the monitoring point at the 5th basement (which was assumed to be 8.0 MN based on the design) to the column load, and the gross load was calculated as 73.4 MN. The estimated gross load was greater than, but roughly agreed with the design column load (67.1 MN). The load carried by the raft (27.4 MN) was obtained using the measured contact pressure (D5) in the tributary area by assuming a uniform distribution of the contact pressure on the bottom surface of the raft. This assumption would be acceptable because the rigidity of the raft is fairly high. Then, the axial load of the pile was calculated as 46.0 MN by subtracting the raft load from the gross load. Note that the pile load in the design was 60.4 MN (67.1x0.90).

Figure 15 shows the ratio of the load carried by the pile to the gross load in the tributary area, together with that to the net load in which the pore-water pressure was assumed to be constant after March 2013 as indicated in Figure 14. Then, the groundwater buoyancy was 17.8 MN. Both the ratios of the pile load were stable after E.O.C. and the ratio to the gross load was estimated to be 0.63 in June 2018, while that to the net load was 0.83.

It should be noted that the load of Pile 4F just before the casting of the foundation slab (which corresponds to the preceding load and was approximately equal to the load of Column 4F (51.6 MN)) decreased after the casting of the slab and reached 46.0 MN in June 2018, as is seen in Figure 14. This indicates that the groundwater buoyancy became greater than the subsequent load after the casting of the slab, i.e., $U_w > (W - W_1 - W_2)$ in the equation (4). By substituting the measured data (P_r=27.4 MN, W_1= 51.6 MN and U_w=17.8 MN) and the estimated values (W=73.4 MN and W_2=8.0 MN) into the equation (5), the value of α_p' is calculated to be 1.4 (>1), which is illogical. However, considering an error in the estimated values and measurements, the value of α_p' could be logical. For example, if considering possible increase in pore-water pressure after the cease of functioning of the piezometer and assuming the buoyancy of U_w=20 MN, α_p' is calculated to be 0.90. Thus, it appeared that the equations (4) and (5) for evaluating the load sharing in the top-down method are reasonable. Furthermore, it was confirmed that the axial load of the pile in the design was fully greater than those estimated based on the field monitoring from the beginning of the construction to 55 months after E.O.C.

6. CONCLUSIONS

Based on the field monitoring on the settlement and the load sharing of piled raft supporting a 300-m high building constructed by top-down method, the following conclusions can be drawn:

(1) The maximum rebound of the ground at the end of the excavation was 47 mm. After the casting of the foundation slab, the settlement of the piled raft due to the subsequent load was 7 mm when about 85% of the gross load in the design was imposed on the foundation. At that time, the settlements at the 1st floor were 28-33 mm which include the vertical displacements of the piles due to the preceding load and those of the piled raft due to the subsequent load, in addition, the axial shrinkage of CFT columns under the 1st floor.

(2) The ratio of the load carried by the pile to the gross load in the tributary area 55 months after E.O.C. was estimated to be 0.63, while the ratio to the net load was 0.83. Thus, the ratio of the load carried by the pile to the net load roughly agreed with the design value (0.90) in which the groundwater buoyancy acting on the raft bottom was neglected on a conservative side. Furthermore, it appeared that the equations (4) and (5) for evaluating the load sharing between the piles and the raft in the top-down method are reasonable through the simulation of the monitoring results. Consequently, it was confirmed that the axial load of the pile was fully greater than those estimated based on the field monitoring.

7. ACKNOWLEDGEMENTS

The authors express sincere gratitude to Mr. K. Akiyama, Mr. M. Nakajima, Mr. S. Kushima, Dr. T. Kono and Mr. Y. Taya of Takenaka Corporation for their contribution throughout the process of foundation design and performing the monitoring.

8. REFERENCES

Building Standard Law of Japan, (2000) Notification No. 1461 of the Ministry of Construction (in Japanese).

Hamada, J., Tsuchiya, T., Tanikawa, T. and Yamashita, K. (2015) “Lateral loading tests on piled rafts and simplified method to evaluate sectional forces of piles”, Geotechnical Engineering Journal of the SEAGS & AGSSEA, Vol.46, No.2, pp. 29-42.

Hirai, Y., Wakai, S. and Aoki, M. (2015) ”In-site pull-out tests of cast-in-place concrete piles with belled enlargements”, 15th Asian Regional Conf. on SMGE, JPN-012.

Ichihara, M. (1993) “Osaka Group”, Sogakusha, 340p (in Japanese).

Katzenbach, R., Arslan, U. and Moormann, C. (2000) “Piled raft foundation projects in German”, Design applications of raft foundations, Hemsley J.A. Editor, Thomas Telford, pp. 323-392.

Kono, T., Sugiura, S., Yamashita, K., Hirai, Y. and Soga, Y. (2008) “Piled raft foundation supporting a 247-m high building”, Kiso-ko, Vol. 36, No. 1, pp. 92-95 (in Japanese).

Poulos, H. G. (2001) “Piled raft foundations: design and applications”, Geotechnique, 51, No.2, pp. 95-113.

Poulos, H. G. and Bunce, G. (2008): "Foundation design for the Burj Dubai -The world's tallest building-", Proc. of 6th Int. Conf. on case histories in Geotechnical Engineering, Paper No. 1. 47.

Research Committee on Geotechnical Information on Osaka Bay. (2002) "Ground and Construction of Bay Area. Association of Research on Geotechnical Information in Osaka Bay", 505+65 pp. (in Japanese)

Tokimatsu, K., Suzuki, H. and Sato, M. (2005) "Effects of inertial and kinematic interaction on seismic behavior of pile with embedded foundation", Soil Dynamics and Earthquake Engineering, Vol. 25, pp. 753-762.

Verdugo, R. (2017) "Seismic site classification", Proc. of the 3rd International Conference on Performance-based design in Earthquake Geotechnical Engineering, PBDⅢ, 526.

Yamashita, K., Yamada, T. and Kakurai, M. (1998) "Simplified method for analyzing piled raft foundations", Proc. of the 3rd Int. Geotechnical Seminar on Deep Foundations and Auger Piles, pp. 457-464.

Yamashita, K., Yamada, T. and Hamada, J. (2011) "Investigation of settlement and load sharing on piled rafts by monitoring full-scale structures", Soils & Foundations, Vol. 51, No. 3, pp. 513-532.

Yamashita, K. and Hamada, J. (2013) "Load sharing behavior of piled raft supporting tall building constructed by top-down method", Proc. of the 18SEAGC & 1AGSSEA, pp. 859-864.